scientific reports

Check for updates

OPEN

Peptides developed against receptor binding sites of the E glycoprotein neutralize tick-borne encephalitis virus

Patrícia Petroušková[1], Katarína Bhide[1], Evelína Mochnáčová[1], Amod Kulkarni[1,2], Jana Jozefiaková[1], Zuzana Tkáčová[1], Tomáš Maľarik[1], Katarína Kucková[1], Lea Talpašová[1], Jakub Víglaský[1], Ádám Kevély[3,4], Kamila Koči[4,5], Eva Nováková[3,4], Juraj Koči[3,5]✉ & Mangesh Bhide[1,2]✉

Infection caused by tick-borne encephalitis virus (TBEV) often manifests with meningitis or encephalitis. Domain III (DIII) of the envelope (E) glycoprotein on the TBEV surface facilitates virion attachment to the cell receptor and initiates cell entry. As a result, this research focused on the DIII to develop antiviral molecules that could prevent cell entry. We first identified two receptor-binding sites (RBS, $_{300}$SGLTYTMCDK$_{309}$ and $_{317}$APTDSGHDTVVMEVTFSGTKPCR$_{339}$) on DIII, that are involved in binding to human brain microvascular endothelial cells (hBMECs). Then we sought to isolate peptides from two combinatorial peptide-phage libraries that bind to the RBS and prevent protein E from attaching to hBMECs. Three cyclic peptides (CP2-CNSSKLHMC, CP20-CDGRPDRAC, CP23-CMKESIRGC) and a linear peptide (LP16-AFHPRQMETQMY) inhibited DIII binding to hBMECs. CP2 and CP20, both non-cytotoxic and hemocompatible, effectively neutralized a live virus. CP2 and CP20 deserve further attention for their potential application as anti-TBEV therapeutics that prevent viral cell entry.

Keywords Tick-borne encephalitis virus, Domain III, Blocking peptides, Phage display, hBMECs, PRNT, Virus neutralization, Combinatorial phage library

Tick-borne encephalitis virus (TBEV), the causative agent of tick-borne encephalitis, causes a severe neurological infection in humans[1]. It is responsible for approximately 10,000 cases per year[2]. In about 30% of TBEV-infected patients, clinical manifestations range from mild fever to severe encephalitis or encephalomyelitis[3]. There has been no TBE-specific therapy available, and vaccines only offer temporary protection against TBE infections. As a result, the development of effective therapeutic molecules, such as antibodies, peptides, or synthetic compounds is highly desirable. Peptides are becoming popular as potential therapeutics to remedy viral infections, owing to their low molecular weight, low toxicity, high specificity, and low production cost[4]. In addition, peptides can effectively target various aspects of a viral infection, e.g. viral attachment, entry, fusion, or replication[5,6]. Notably, a cell-entry inhibition based on the blocking of viral attachment protein has become a progressive antiviral strategy[7,8]. The discovery of such peptides is allowed by the utilization of high-throughput screening technology coupled with a generation of highly diverse libraries, such as combinatorial phage display. Combinatorial libraries are simple to use, commercially available[9], usually consist of only 6 to 15 amino acids[10], and have already been used to develop antiviral peptides[10–15].

TBEV enters the CNS without affecting the integrity of the endothelial layer of the blood-brain barrier (BBB)[16,17]. Human brain microvascular endothelial cells (hBMECs), a luminal component of the BBB, represent a primary barrier against viral dissemination into the CNS. The cells are sensitive to TBEV infection and may facilitate TBEV entry into the brain[16]. The initial steps in the flavivirus life cycle (attachment and cell-entry) are

[1]Laboratory of Biomedical Microbiology and Immunology, The University of Veterinary Medicine and Pharmacy in Košice, Komenského 73, 04181 Košice, Slovakia. [2]Institute of Neuroimmunology of Slovak Academy of Sciences, 84510 Bratislava, Slovakia. [3]Department of Virus Ecology, Institute of Virology, Biomedical Research Center, Slovak Academy of Sciences, Dúbravská cesta 9, 84505 Bratislava, Slovakia. [4]Department of Microbiology and Virology, Faculty of Natural Sciences, Comenius University, Ilkovičova 6, 84215 Bratislava, Slovakia. [5]Institute of Zoology, Slovak Academy of Sciences, Dúbravská cesta 9, 84506 Bratislava, Slovakia. ✉email: juraj.koci@savba.sk; bhidemangesh@gmail.com

mediated by envelope (E) glycoprotein[18,19], which consists of 3 distinct domains (DI to DIII)[20,21]. DIII is the major antigenic domain with a significant role in the cell receptor attachment[22–26]. Therefore, the E glycoprotein with its DIII represents an ideal target for the development of entry-inhibiting peptides.

We believe that the entry-inhibiting strategy could be based on peptides specifically binding the receptor-binding sites (RBSs) on the viral DIII. In our recent study, we established an experimental pipeline to map plausible RBSs on DIII of West Nile virus (WNV) using a proteomic approach[27]. The present study employed the same technique to map RBSs on DIII of TBEV and use them to select RBS-blocking peptides. Two RBS $_{300}$SGLTYTMCDK$_{309}$ and $_{317}$APTDSGHDTVVMEVTFSGTKPCR$_{339}$ were revealed. Combinatorial phage libraries displaying structurally constrained 7-mer peptides (with a disulfide bond) and 12-mer linear peptides were panned against recombinant DIII (rDIII) and recombinant RBSs were used to elute peptides bound on rDIII (competitive elution). Six blocking peptides were shortlisted, produced in soluble form, and tested for their ability to inhibit the interaction between DIII and hBMECs, followed by non-toxicity and finally the ability to neutralize the live virus. CP2 (CNSSKLHMC) and CP20 (CDGRPDRAC) showed no cell toxicity or hemolysis, neutralized the virus, and reduced hBMECs infection by 95% and 88%, respectively.

Results and discussion

rDIII interacts with hBMECs

Endothelial cells of the brain vasculature represent a primary barrier against CNS invasion, however, its evasion by TBEV was documented earlier[16]. Therefore, the hBMECs were selected as target cells in this study. It is supposed that the adhesion of TBEV to the brain endothelium, mediated through DIII, is a pivotal step in neuroinvasion[28]. DIII, overexpressed in *E. coli* and purified by chromatography, had ~ 12 kDa (Fig. 1a–c) and showed binding affinity to proteins of hBMECs immobilized in an ELISA plate (Fig. 1d) and intact endothelial cells in immunocytochemistry (Fig. 1e).

Receptor binding sites on DIII

Receptor binding sites on DIII were mapped using the method described in our previous publication[27], which relies on the immobilization of the receptor/s on the substrate, formation of receptor-ligand complex, digestion of the complex with protease, retrieval of bound peptides of ligands from the immobilized receptor and identification of peptides by MALDI-TOF-MS. Two amino acid sequences $_{300}$SGLTYTMCDK$_{309}$ (~ 1118 Da; RBS-1) and $_{317}$APTDSGHDTVVMEVTFSGTKPCR$_{339}$ (~ 2435 Da; RBS-2) were identified using above-mentioned approach (Fig. 2a–e). To be recognized as potential RBSs, both peptides must be able to attach to endothelial cell receptors. The recombinant form of both RBSs produced in this study (Fig. 3a–d, RBS-1 and RBS-2) retained affinity to proteins of endothelial cells and fixed endothelial cells in ELISA and immunocytochemistry, respectively (Fig. 3e, f), implying that both peptides are involved in E protein-cell interaction and may be a part of a receptor-binding pocket.

Previously, key regions of the E glycoprotein involved in the virus's biology were investigated by various researchers[20,29–33]. Using site-directed mutagenesis, four amino acids (D308, K309, T310, and K311) located on the upper lateral surface of DIII were identified as potential receptor binding sites[29], of which D308 and K309 are present in RBS1 $_{300}$SGLTYTMCDK$_{309}$ (Fig. 2c, d). Variations in these amino acids affect heparan sulfate binding and even virulence[20,29,34], thereby highlighting their role in the ligand-receptor interaction. It was reported that mutation of H319 in Japanese encephalitis virus (JEV) DIII, which is equivalent to H323 in TBEV DIII, significantly reduced the virus entry[30]. The identification of $_{317}$APTDSGHDTVVMEVTFSGTKPCR$_{339}$ as a plausible RBS in our experimental approach, which includes H323 (Fig. 2e), suggests that this region may be another important receptor-binding determinant. The spatial relationship between D308 to K311 and residue F332 was previously revealed[29], demonstrating that F332 is located immediately behind the residues K308-K311, allowing RBS1 and RBS2 to be presented close together and form a receptor-binding pocket. The crystal structure of the E protein of TBEV (PDB: 1SVB) also supports the fact that RBS1 and RBS2 potentially form a pocket, and while RBS-1 is fully surface exposed (available to bind cell receptors), the RBS-2 ($_{317}$APTDSGHDTVVMEVTFSGTKPCR$_{339}$) is partially surface-exposed with C-terminal residues FSGT (Fig. 2c, d).

Peptides from combinatorial libraries screened against RBSs of rDIII

Given E glycoprotein's key receptor-binding function, we aimed to isolate peptides from combinatorial phage libraries to find mid-sized molecules that can bind the RBS on DIII, reduce interaction with cells (particularly brain endothelium), and possibly block virus cell-entry. Combinatorial peptide-phage libraries allow for high-throughput screening of linear and structurally constrained peptides to isolate unique molecules with specific affinity for the target. To date, several antiviral peptides targeting the E protein or DIII of various flaviviruses have been generated[11,15,35–37]. However, to our knowledge, no phage-derived peptides have been reported against TBEV. As a result, both combinatorial loop-constrained heptapeptide and linear dodecapeptide phage libraries were screened in the current study. We used a combination of imidazole (to elute the rDIII-phage complex specifically) and a molar excess of purified RBSs to ensure competitive elution of RBS-binding phages only during the rounds of biopanning. Each round of panning resulted in a gradual increase in target-binding phage clones (Supplementary Fig. 1), and phages from the final round of panning demonstrated binding affinity to rDIII (Supplementary Fig. 2). Sequencing of the phage clones isolated from the last round of panning revealed enrichment of the phages displaying peptides that could have significant binding affinity to DIII, as the sequences were segregated into six groups in the case of phages displaying cyclic peptides and twelve in the case of linear peptides (Fig. 4a). Bioinformatic analysis of peptide sequences revealed that none of the peptides matched with any known TUP motifs (so-called target-unrelated peptide) or other previously characterized peptides deposited in the UniProtKB database (Supplementary Table S1), indicating that the peptides displayed on phages might be target-specific and might not be enriched as a result of non-specific interaction during panning. The target-

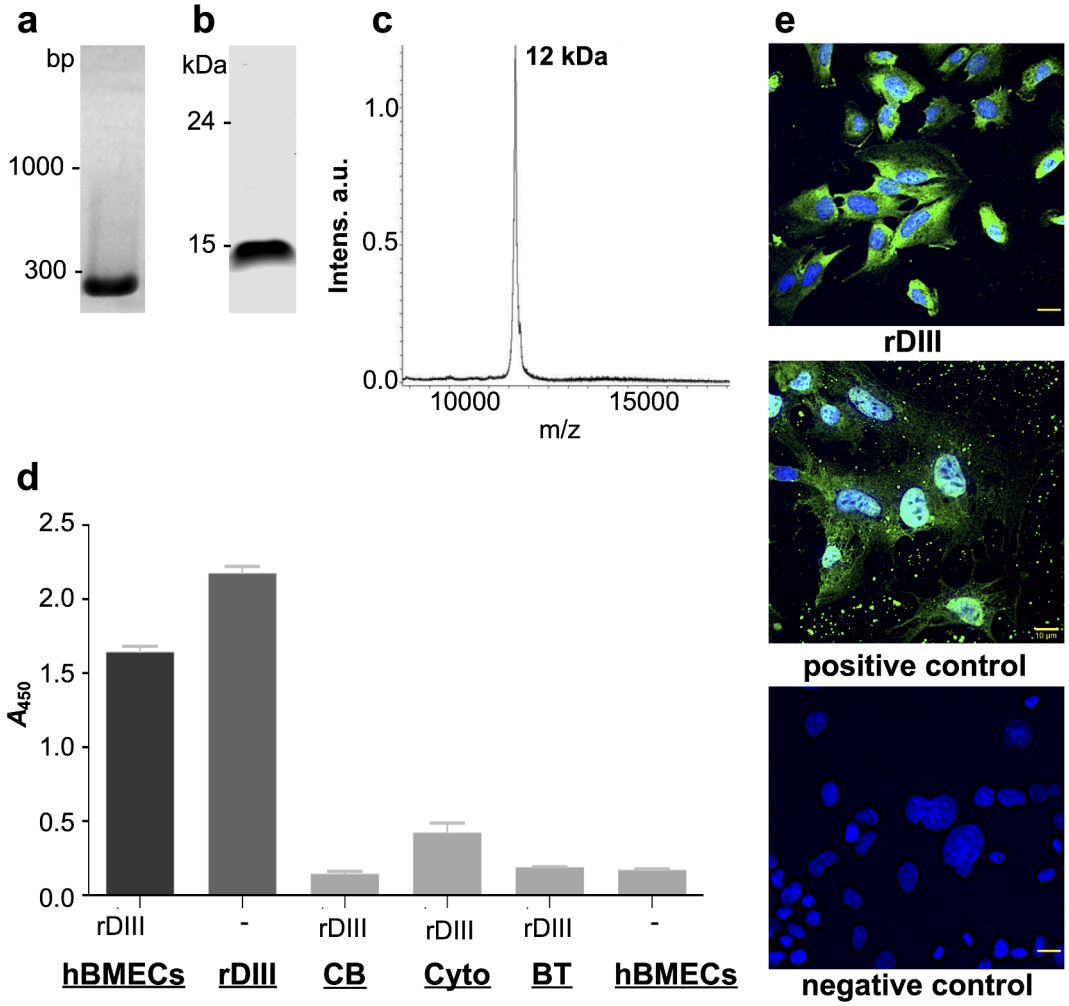

Fig. 1. Production of rDIII and its binding to hBMECs. (**a**) Amplicon of the gene fragment encoding DIII resolved on agarose gel. (**b**) Purified rDIII separated with LDS-PAGE. (**c**) The molecular mass of rDIII was confirmed by MALDI-TOF-MS. The observed mass of rDIII is [M + H]+. The observed molecular weight of rDIII (12 kDa) was consistent with the theoretical molecular mass predicted using Geneious Pro software. (**d**) Interaction between rDIII and proteins of hBMECs assessed by ELISA. The interaction was detected with the HisProbe-HRP conjugate. Underlined reagents were coated into the microtiter wells. Data present means of triplicates with ± S.D. *A* absorbance, *hBMECs* whole cell protein extract of hBMECs. As negative control wells were coated either coating buffer only (CB) or with cytoplasmic fraction of the hBMECs (Cyto) or with proteins from bovine turbinate endothelial cells (BT). As negative reaction, rDIII was excluded from the reaction (indicated by –). (**e**) Binding of rDIII on cultured hBMECs by immunocytochemistry. Bound rDIII was detected with FITC anti-6xHis tag antibody. Nuclei are stained with DAPI. The assay was performed in biological triplicates. Positive control—an unrelated protein known to interact with endothelial cells (MafA of *Neisseria meningitidis*); negative control—rDIII was excluded from the assay.

binding of individual phage clones was also confirmed in ELISA (Fig. 4b, c). Clone LP20, however, exhibited a strong signal in ELISA when rDIII was excluded, suggesting that LP20 is TUP and may bind non-specifically to plasticware. The phage clones (CP2, CP20, CP23, LP16, LP19, and LP21) that showed absorbance in ELISA $A_{450} > 1.5$ (Fig. 4b, c) were shortlisted, and peptides displayed by them were produced.

Recombinant peptides maintain the ability to bind rDIII

The peptides were overexpressed in *E. coli*, purified by chromatography, and digested by enterokinase (to remove the N-terminal 6xHis-28aa-GGGGS tag). Peptides had molecular masses between 1.352 kDa and 1.797 kDa, which corresponded to their predicted molecular weights (Fig. 4d–g, Supplementary Fig. S3). Because the 7-mer peptides are displayed on the phage pIII protein in cyclic form, maintaining cyclization is essential for peptide folding, and thus activity and functionality. *E. coli* strains, routinely used for protein production are not always successful in protein folding due to the absence of post-translational modifications. Therefore, to accomplish the formation of the disulfide bonds, peptides were overexpressed in a genetically engineered *E. coli* Shuffle express strain, which promotes disulfide bond formation in the oxidizing cytoplasmic environment. Thiol-reactive

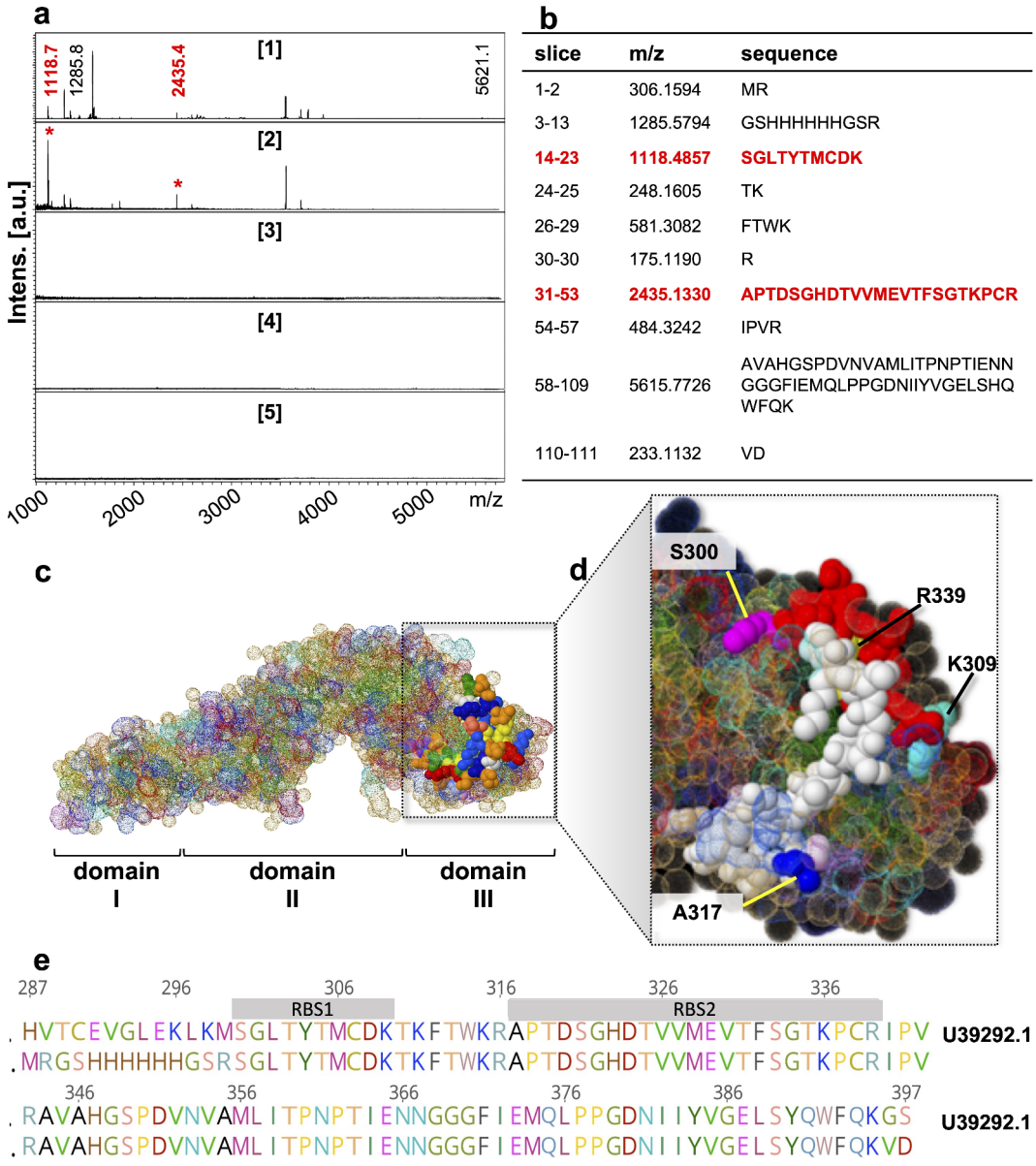

Fig. 2. Receptor binding sites on DIII. (**a**) Isolation of RBSs of DIII using on-membrane limited tryptic digestion. Lane (1) MALDI-TOF-MS spectrum of in-solution limited tryptic digestion (60 min) of rDIII. Lane (2) hBMECs proteins were immobilized on PVDF membrane, allowed to interact with rDIII, complex was trypsinized, and bound peptides of rDIII to hBMECs were retrieved and identified on MALDI-TOF-MS. Lane 3–5. Negative controls were generated by omitting tryptic digestion of the complex (lane 3) or rDIII (lane 4) or hBMECs (lane 5) from the protocol. (**b**) List of theoretical peptides of DIII predicted by in silico tryptic digestion using mMass software V 1.0 (http://www.mmass.org/). Peptides identified from on-membrane limited proteolysis of rDII-hBMECs complex (in panel **a** *) matching with in-solution digestion of the ligand and theoretical masses are colored red in panels (**a**) and (**b**). Please note that the predicted masses of the peptides are [M + H]+. The observed masses of the peptides are also [M + H]+. No peptides were found to be leached in negative controls, which acknowledged the mapped RBSs on DIII. (**c**) Crystal structure of the E protein of TBEV (PDB accession number 1SVB), in which identified RBSs are highlighted. (**d**) Zoom in on the DIII. RBS1 is in red, RBS2 is in white. (**e**) Amino acid sequence alignment of rDIII TBEV used in the study (lower sequence in the alignment) with the sequence of the E protein of TBEV deposited under U39292.1 in the GenBank.

maleimide labeling of cysteine residues in purified CPs was only possible when they were reduced with tris(2-carboxyethyl)phosphine, not when they were oxidized (Fig. 4h), confirming the presence of disulfide bonds in CP2, CP20, and CP23, and thus their cyclic structure.

Screening of the loop-constrained peptide libraries (like the C7C-mer library) readily generates peptides with a higher affinity and specificity to the target[38–42]. Moreover, cyclic peptides demonstrate a lower conformational entropy, which increases the probability that they will retain their binding capacity when removed from the

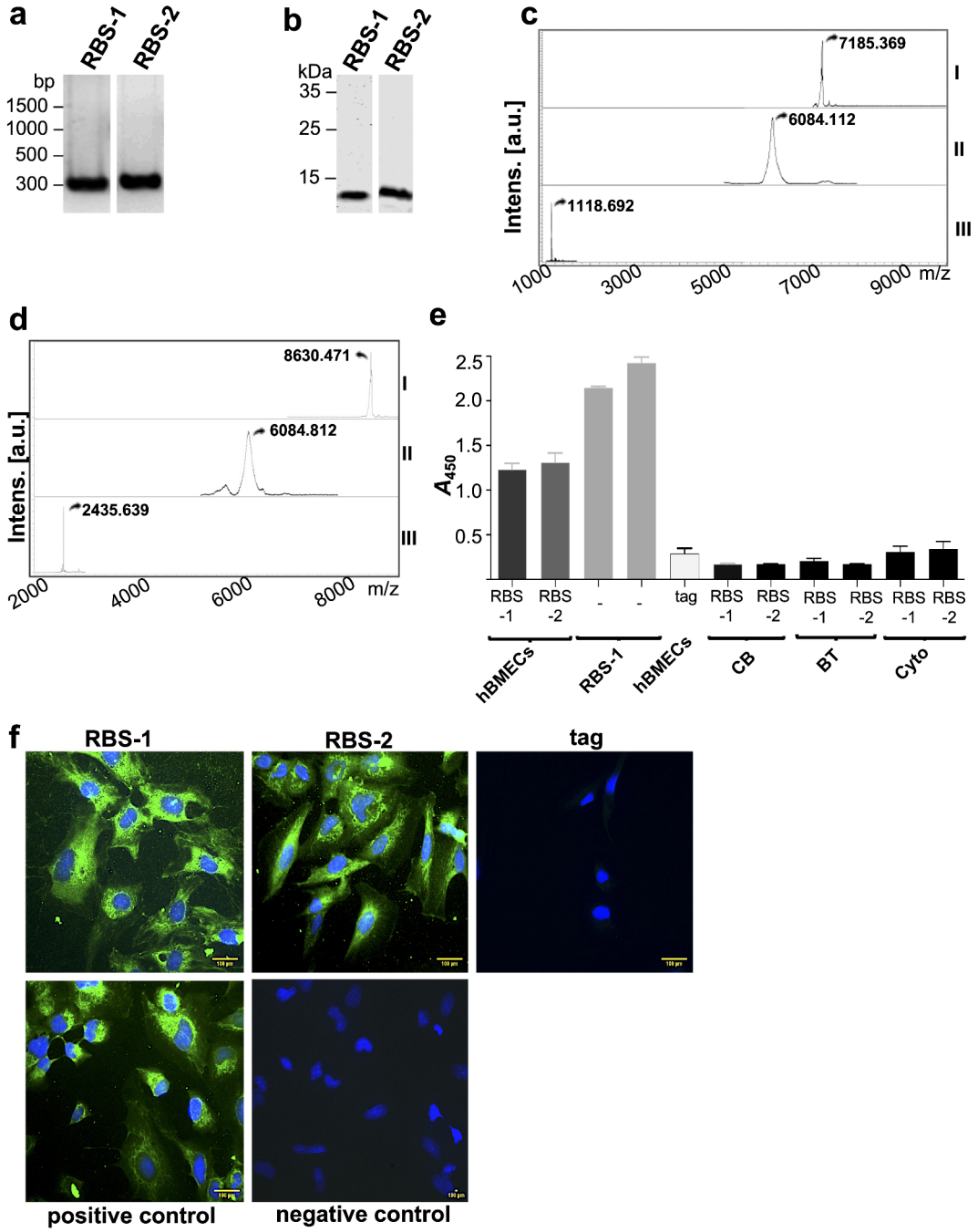

Fig. 3. Production of RBSs and their binding to hBMECs. (**a**) Amplicons encoding tagged RBSs resolved on agarose gel. (**b**) Purified tagged RBSs resolved on LDS-PAGE. RBS-1 (panel **c**) and RBS-2 (panel **d**) detected by MALDI-TOF-MS. In both (**c**) and (**d**): *I* tagged RBS; *II* the N-terminal solubility tag after digestion with enterokinase; *III* purified RBS after removal of the tag. The observed molecular masses of tagged RBS-1 (7185.369 Da) and tagged RBS-2 (8630.471) were matched with theoretically predicted masses (7185 Da and 8630 Da respectively). The molecular masses of RBSs after removal of the tag correspond to the identified RBSs (~ 1118 Da and ~ 2435 Da). (**e**) Validation of the interaction between RBSs and protein of hBMECs assessed by ELISA. The interaction was detected with the HisProbe-HRP conjugate. Reagents in bold were coated into microtiter wells. hBMECs—protein extract of hBMECs; the tag—6.2 kDa solubility tag. As negative control wells were coated either coating buffer only (CB) or with cytoplasmic fraction of the hBMECs (Cyto) or with proteins from bovine turbinate endothelial cells (BT). Data present means of triplicates with ± S.D. (**f**) Validation of the binding of RBSs on cultured hBMECs by immunocytochemistry. Nuclei are stained with DAPI. Positive control—rDIII was incubated with the cells. Negative control—RBSs were excluded from the assay. The N-terminal solubility tag was incubated with the cells and no interaction was detected (this served as additional negative control). The assay was performed in triplicates. Scale bar—10 µm.

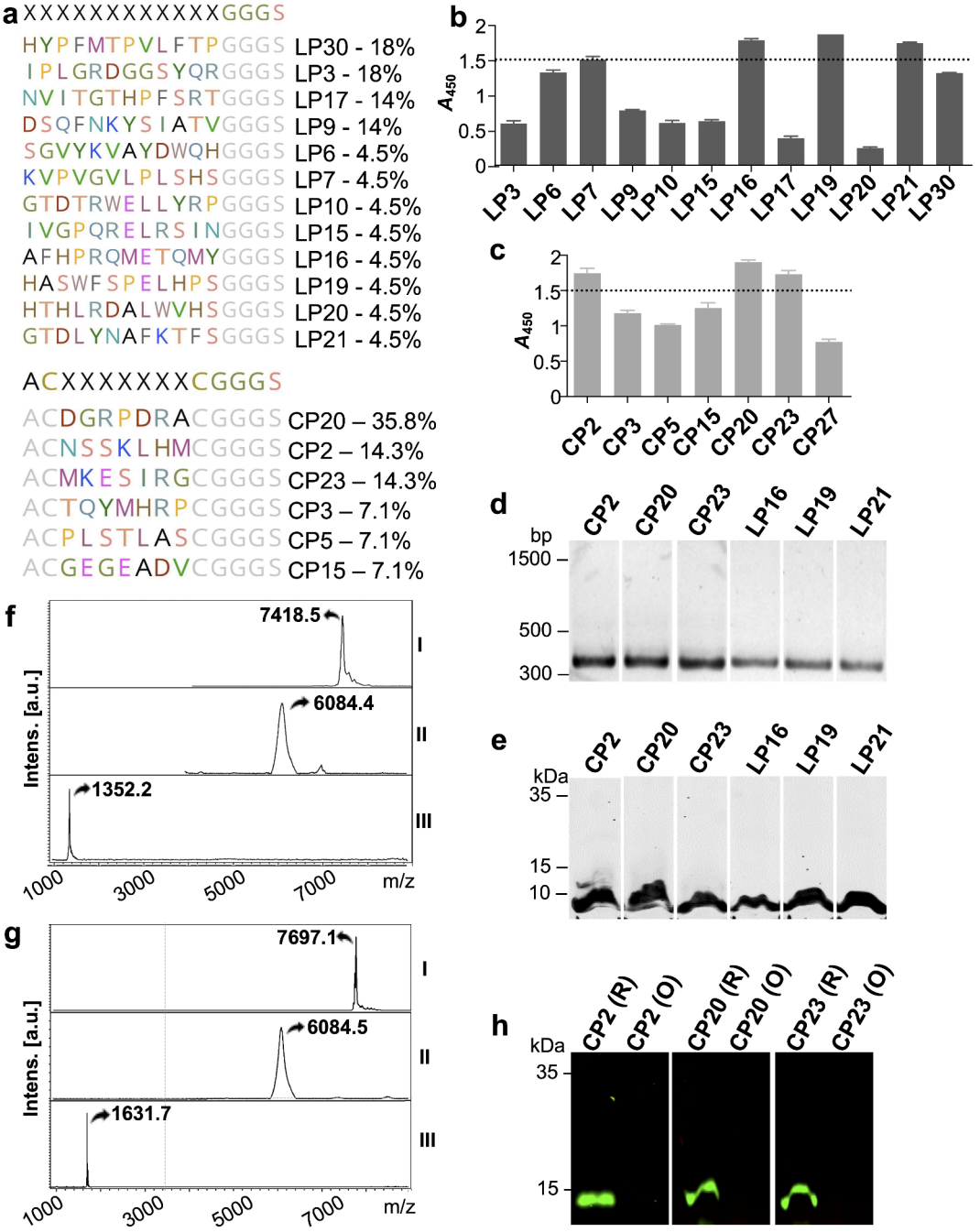

Fig. 4. Peptides against RBSs isolated from combinatory phage libraries and production of best RBS-binders. (**a**) Phage clones separated from the last round of biopanning and sequenced. Amino acid sequences deduced from DNA sequences are aligned for clones from linear (upper panel) and cyclic peptide (lower panel) libraries. Sequences were grouped according to homology, and a representative sequence from each group is presented. The number of sequences present in each group are depicted in percentage. (**b**, **c**) Interaction of individual phage clones (displaying linear peptides—(**b**) and cyclic peptides—(**c**) with rDIII immobilized in ELISA wells. As a negative control, each phage clone was incubated in an empty well blocked with BSA. Values presented here are means of triplicates with ± S.D after subtraction of absorbance observed in negative control. (**d**) Amplicons encoding tagged peptides resolved on the agarose gel. (**e**) Purified tagged peptides on LDS-PAGE. (**f**,**g**) Molecular masses of the representative peptides (cyclic CP2—**f** and linear LP21—**g**) confirmed by MALDI-TOF-MS. In both (**f**) and (**g**) *I* N terminal tagged peptide; *II* the tag after enterokinase digestion; *III* purified peptide after removal of the tag. (**h**) The cyclic form of 7-mer peptides was confirmed. Any free thiols present in the tagged peptides were blocked with *N*-ethylmaleimide (NEM). Peptides were then either reduced (R) or maintained in oxidized form (O). Both R and O forms were incubated with thiol-reactive maleimide and then separated on non-reducing LDS-PAGE., If thiols in the peptide are occupied with the disulfide bond, they remain unblocked and get reduced with TCEP. Free thiols in reduced peptides are then labeled giving a green signal. In the oxidized form, no free thiols are available, thus no labeling occurs (no green signal).

phage context. Although linear peptides allow for many conformations and adaptability to various structures, this flexibility may reduce their affinity for the target[43]. As a result, we anticipated that the binding of CPs to rDIII would differ significantly from that of LPs. Although cyclic peptides (A_{450} > 2.2) showed more affinity to rDIII than linear peptides (A_{450} > 1.6, Fig. 5a), the difference was not statistically significant (two-tailed paired Student's *t*-test, $p < 0.01$).

CPs and LPs restricted the binding of rDIII to the endothelial cells

To see if CPs and LPs could reduce the interaction between rDIII and hBMECs proteins, rDIII was pre-incubated with peptides and then allowed to interact with hBMECs proteins or intact endothelial cells. All peptides (CP2, CP20, CP23, LP16, LP19, and LP21) significantly ($p < 0.01$, two-tailed paired Student's *t*-test) restrained the binding of rDIII to endothelial cell proteins, tested with blocking-ELISA (Fig. 5b). When rDIII was pre-incubated with CP2, CP20, and CP23, it completely lost binding to cultured hBMECs. However, rDIII retained a partial affinity when pre-incubated with LP16, but appeared to maintain binding ability when pre-incubated with LP19 or LP21 (Fig. 5c). It is not surprising that peptides LP19 (HASWFSPELHPS) and LP21 (GTDLYNAFKTFS), which have a good rDIII binding affinity in ELISA (A_{450} > 1.5; Fig. 5a) and a promising capacity to block interaction between rDIII and cell lysate of BMECs in blocking-ELISA, could not completely inhibit binding of rDIII on intact endothelial cells in immunocytochemistry (Fig. 5c). One explanation is that those peptides do not occupy the RBSs sufficiently to inhibit rDIII-receptor interaction when the receptors are in their native conformation on the cell surface. Therefore, LP19 and LP21 were excluded from further investigation.

DIII-blocking peptides are not toxic

The ideal antivirals are specific for virus-related processes and non-toxic to host cells. Since several peptides with therapeutic potential often exhibit undesired cell toxicity[44,45], DIII-blocking peptides (CP2, CP20, CP23, and LP16) were tested for their cytotoxicity and hemolytic activity. Cell viability > 70% compared to untreated control (ISO 10993-5: Tests for in vitro cytotoxicity) and < 10% hemolysis[46] define a peptide as a safe candidate for translation to the therapy. Even at a concentration of 6 µM, neither of the peptides significantly ($p < 0.01$, two-tailed unpaired *t*-test with Welch's correction) affected hBMECs metabolism when monitored with XTT (Fig. 6a) nor showed hemolytic activity (hemolysis < 0.14% after 1 and 5 h of incubation, Fig. 6b). However, CP23 and LP16 were excluded from further investigation due to their slightly negative effect on cell viability (85% and 83% respectively at 6 µM).

CP2 and CP20 efficiently inhibit cell-entry of TBEV in BHK21 and hBMECs

As CP2 and CP20 peptides were found to be target-specific and safe for cell culture, the final evaluation focused on their ability to inhibit a live virus in vitro. The Hypr strain of TBEV, pre-incubated for 60 min with 1 µg of CP2 or CP20, was unable to infect BHK21 cells. No plaques were observed in the monolayer even after 3 days post-infection (dpi), indicating that both peptides completely neutralized the virus (Fig. 6c). In the control reactions, hyperimmune serum completely neutralized the virus, whereas in virus control (no neutralizing agent was added to the virus), an average of 51 plaques were counted (Fig. 6c).

Based on the preliminary results of the neutralization assay described above, we planned to determine whether both peptides can inhibit viral infection in brain microvascular endothelial cells. Although TBEV can infect endothelial cells in the brain microvasculature, it does not produce the evident cytopathic effect required to form defined plaques. Thus, an alternative approach was used, in which the virus pre-incubated with a peptide was allowed to infect hBMECs and incubated until virus replication peaked. Afterward, the number of viruses released in the hBMECs culture was counted by transferring the medium to the BHK21 monolayer on which plaques were formed (Fig. 7a). The peak of infection in hBMECs was determined by replication dynamics, in which a ten-day-incubation period of the cells infected with TBEV showed a sharp increase of the mean viral titer (pfu/ml) with onset at 1 dpi (15.5 ± 0.5) and culmination at 3 dpi (32750 ± 250) with a continuous but gradual decline towards day 10 dpi (340 ± 25) (Fig. 7c). Similar trend of infection dynamic was reported for Zika virus in hBMECs in which cytopathic effect was absent for up to more than 9 dpi[47]. Even without apparent cytopathic effect, viruses may often profoundly impact the physiology of endothelial cells[48], despite endothelial integrity required for viruses to successfully cross the BBB, as reported for Zika virus infection[49].

The viral plaque reduction assay revealed a full 100% reduction in viral plaque numbers for CP2 and CP20 (Fig. 7b), after preincubation with only 0.8 nM or 1.7 µM (0.62 µg–0.31 µg in 50 µL of suspension containing 20 pfu) of the peptides, respectively, indicating an effective and specific saturation of the DIII-binding sites. Our data are in agreement with recent studies reporting on the virus-neutralizing capacity of small peptides derived from E protein epitopes of several flaviviruses[11,35,50]. Moreover, peptides targeting (i) herpes simplex virus proteins to interrupt a virus-host membrane interaction[51], (ii) Crimean-congo hemorrhagic fever virus to inhibit viral membrane fusion[52], or (iii) reovirus-activated host signaling molecules (JNK and caspase-3 in the CNS) to reduce a lethal viral challenge[53] are further solid examples of peptides' therapeutic potential.

DIII and its blockers: perspectives

The DIII of flaviviruses is an immunoprotein-like domain targeted by antibodies that peak early after infection, and last for several months. A low propensity to cross-reactivity with other flaviviruses[54] may help to avoid an antibody-dependent enhancement of infection. As a result, the DIII domain is frequently selected for developing flavivirus-specific antibodies and blocking inhibitors. So far, several virus-neutralizing antibodies against DIII have been isolated or developed[54–60], among which 7B3[57] recognizes ZIKV DIII residues T335 and G337. The antibody (DENV1-E106), which completely protects against DENV1 infection[58], recognizes the lateral ridge of DIII (DENV1, K307 to K310; K325 to Y326), and monoclonal antibody isolated from DIII-immunized mice

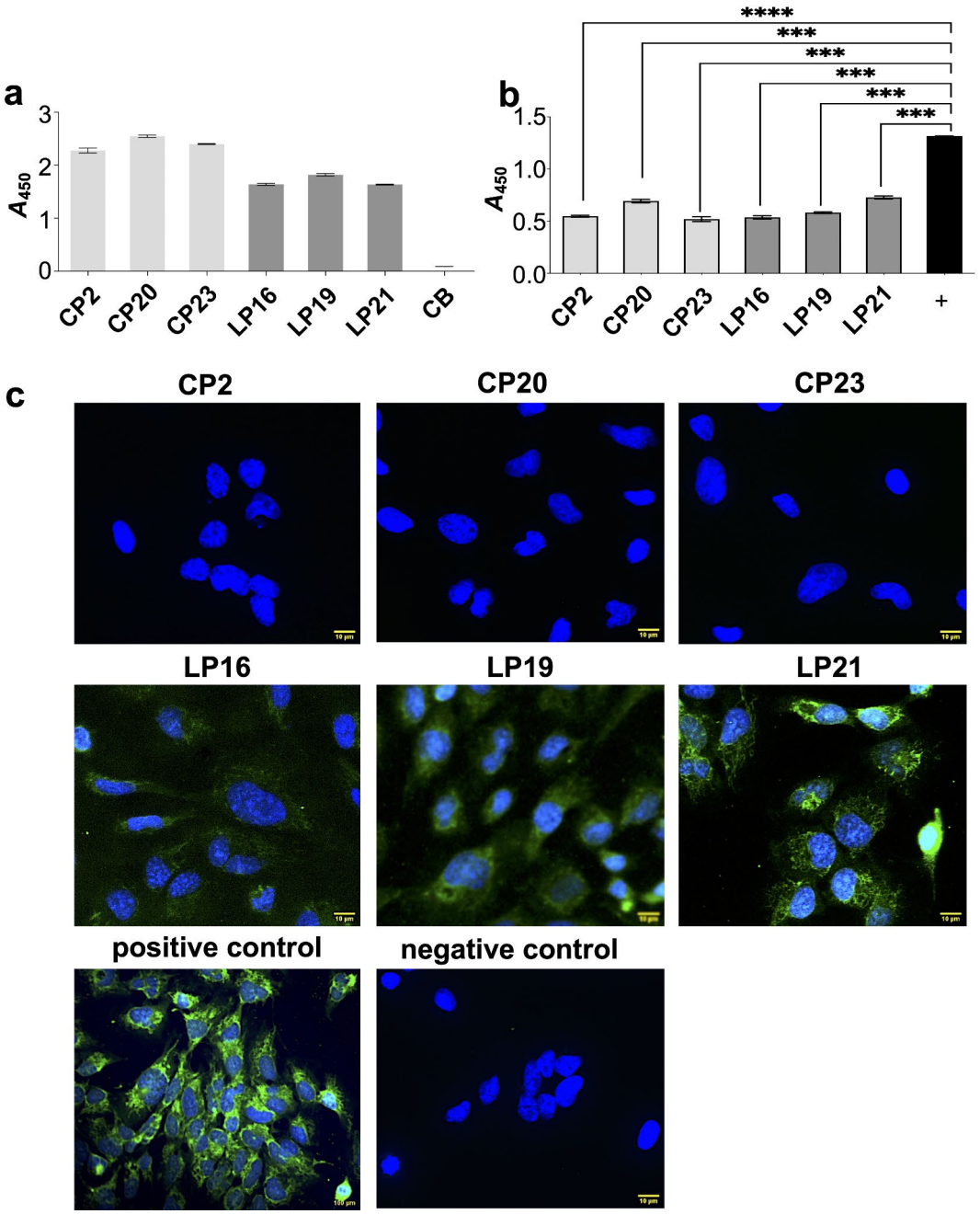

Fig. 5. Blocking of interaction between rDIII and hBMECs by cyclic and linear peptides. (**a**) Affinity of CPs and LPs peptides to rDIII was assessed by ELISA. Peptides (N-tag removed) were immobilized in CovaLink NH plates and allowed to interact with rDIII. The interaction was detected with HisProbe-HRP conjugate and TMB substrate. Data present the mean of triplicates with ± S.D after subtraction from negative control (rDIII was excluded from the assay). The statistical difference between the CPs and LPs was calculated using a two-tailed paired Student's *t*-test ($p < 0.01$). No statistically significant difference was observed. Statistical analysis was performed using GraphPad Prism software v.8.4.3. CB—peptides were replaced by coating buffer in the assay (negative control) to see if rDIII is attaching to the well non-specifically. (**b**) Blocking of the interaction between proteins of hBMECs and rDIII. hBMECs proteins were coated in the ELISA well and then rDIII, preincubated with each LP or CP was added. Inhibition of the interaction was detected by HisProbe-HRP conjugate. Data present the mean of triplicates with ± S.D after subtraction from negative control (rDIII excluded from the assay). A statistically significant difference ($p < 0.01$, two-tailed paired Student's *t*-test) was calculated compared to the positive control (+ interaction between rDIII and hBMECs proteins). **** < 0.0001, *** ≥ 0.0001; CP2: $p < 0.0001$; CP20: $p = 0.0008$; CP23: $p = 0.0009$; LP16: $p = 0.0004$; LP19: $p = 0.0001$; LP21: $p = 0.0002$. (**c**) Blocking of the adhesion of rDIII on cultured endothelial cells. 0.2 nM of rDIII was pre-blocked with a 10-fold molar excess of peptides before incubation with the cells. Any bound rDIII was detected with FITC anti-6xHis tag antibody. Positive control—rDIII was incubated with the cells. Negative control—rDIII was excluded from the assay. Nuclei are stained with DAPI. Bar scale in yellow—10 µm. The assay was performed in biological triplicates.

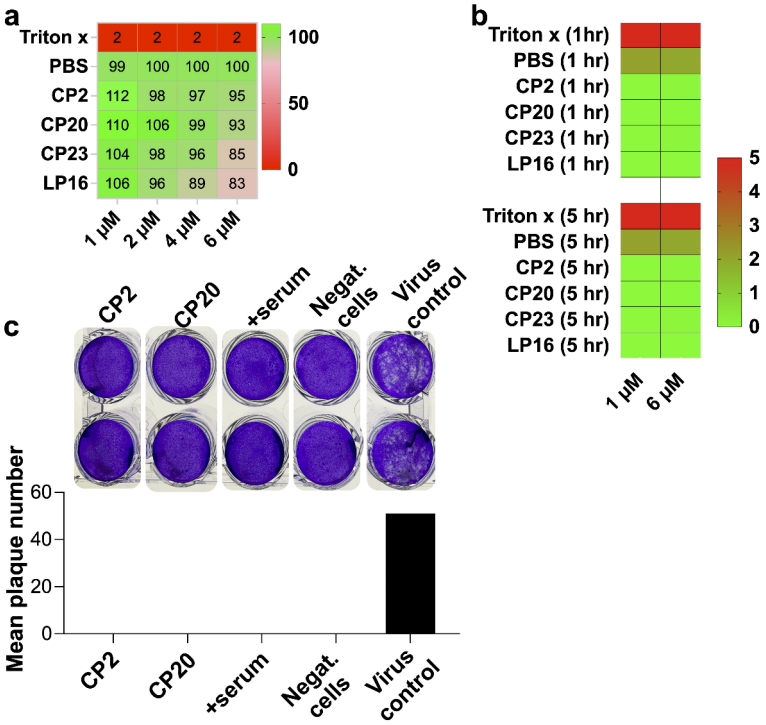

Fig. 6. Toxicity of peptides and their ability to neutralize virus. (**a**) Cytotoxicity of peptides on endothelial cells assessed by XTT after 24 h of incubation at different concentrations (1 µM, 2 µM, 4 µM, and 6 µM) performed in replicates. The statistical difference between treated and untreated cells was calculated by two-tailed unpaired *t*-test with Welch's correction ($p < 0.01$). None of the peptides showed significant cytotoxicity (cell viability < 70%). Statistical analysis was performed using GraphPad Prism software v.8.4.3. PBS—negative control (5 µL of PBS added to hBMECs). Triton x—positive control (cells treated with 0.1% Triton X-100). (**b**) Assessment of hemolytic activity of peptides. Suspension of sheep erythrocytes was incubated with peptides at two different concentrations (1 µM and 6 µM) at two different time points (after 1 h and 5 h). The release of oxyhemoglobin was measured at 414 nm. No hemolytic effect (no release of hemoglobin) of peptides was observed (hemolysis < 0.14%). PBS - negative control (5 µl of PBS added to sheep erythrocytes). Triton x—positive control (0.1% Triton X-100 was added). (**c**) Virus neutralization test. The virus was preincubated with 1 µg of CP2 or CP20 or hyperimmune serum (+serum) or PBS (negat. cells) for 1 h and then allowed to infect BHK-21 cell monolayer for 3 days. Any plaques formed were counted under a microscope and compared with plaques observed in virus control wells (no virus was added to the monolayer). Assay performed in technical duplicate in BSL-3 biocontainment facility.

recognizes amino acid residue between 309 and 320[61]. These findings suggest that the N-terminal region of DIII (amino acid residues 300 to 339), which includes both RBSs as observed in our study, is an important epitope and an attractive region for developing antiviral peptides. Cell entry-inhibiting peptides were derived previously from phage display libraries, for example, P1 and P3 peptides inhibiting JEV infection[35,36], P9 inhibiting WNV[11], and a cyclic 19-amino acid moiety inhibiting Zika virus infection[62]. In addition to these molecules, peptides from animals, plants, or synthetic peptide-based molecules have been successfully tested as cell-entry inhibitors against Dengue virus, Zika virus, and herpes simplex virus type 1[63–66].

Along with previous reports and our promising data showing effective TBEV entry inhibition in hBMEC, it seems obvious that virus or host-derived entry-inhibiting peptides will be at the forefront of specific antiviral therapy research. As there are no clinically approved flavivirus entry inhibitors, and to our knowledge, there are no entry inhibitors developed against TBEV yet, we believe that the peptides developed by us possess the potential to be translated into molecules suitable for preclinical trials.

Methods

Cell culture

Human brain microvascular endothelial cells (hBMECs, Merck, Czech Republic) were cultured following standard procedures for cell culture techniques, details are described in Supplementary Method S1. Bovine turbinate (BT) endothelial cells (ATCC, USA) were cultured in Dulbecco's Modified Eagle's Medium containing 10% horse serum.

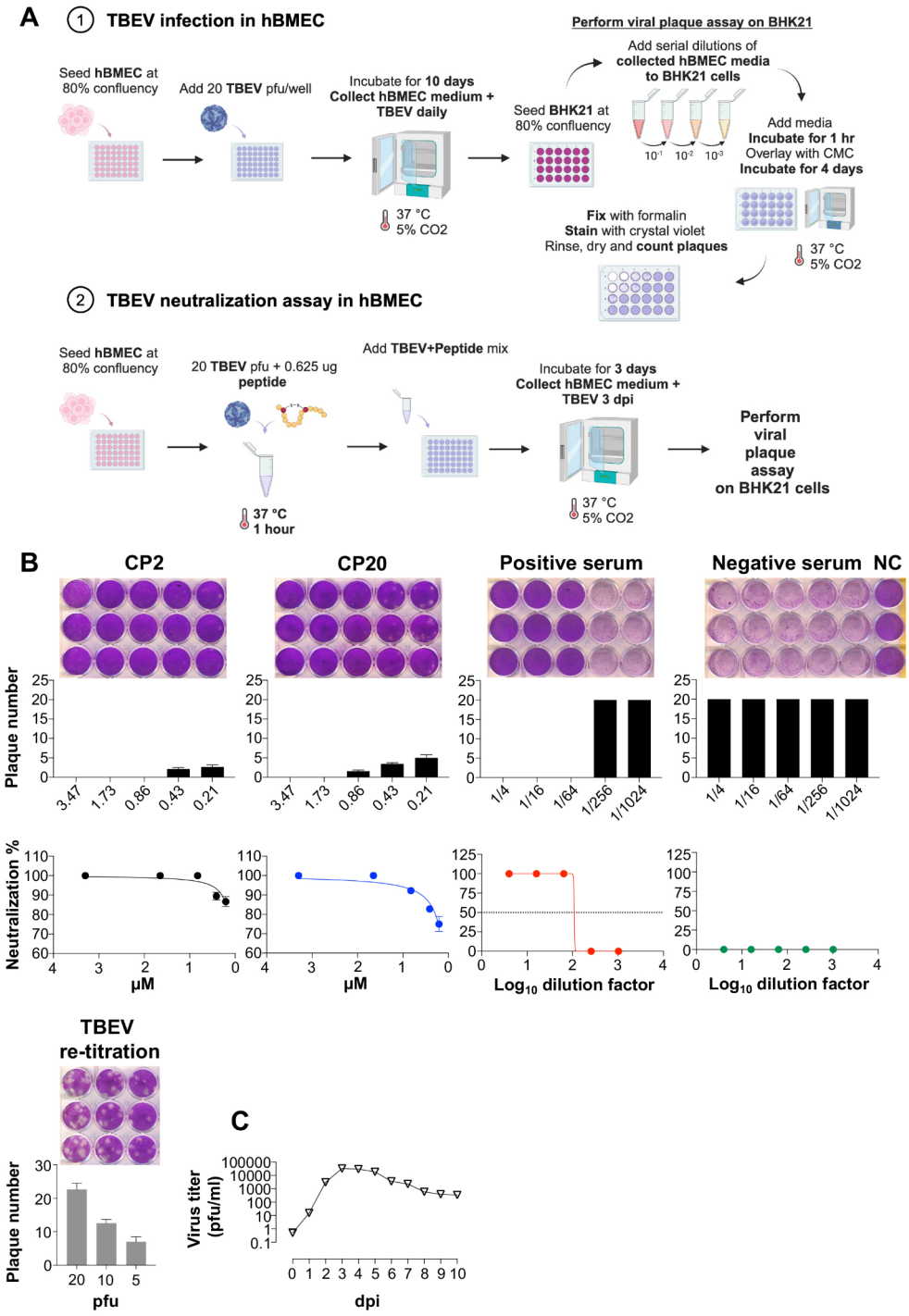

Fig. 7. Peptides CP2 and CP20 efficiently inhibit TBEV replication in vitro. (**a**) Experimental design scheme showing the methodology of TBEV neutralization assays. *CMC* carboxymethylcellulose. Scheme drawing was prepared using Biorender (https://www.biorender.com). (**b**) Dose-dependent TBEV neutralization by C2 and C20 peptides in hBMEC. Presented are images of stained BHK21 cells infected with 3 dpi-hBMEC supernatants incubated with TBEV + C2, TBEV + C20, TBEV + TBEV-positive serum or TBEV + TBEV-negative serum in technical triplicates and three biological replicates (a representative plaque titration assay images are shown). *NC* TBEV-negative cells. The plots below the plaque images show respective mean plaque numbers and virus neutralization values, the calculation of which can be referred to in the Methods. The degree of the virus neutralization by the peptides and sera is expressed as a dose-dependent nonlinear fit curve. 50% neutralization threshold is indicated by a dashed line. TBEV re-titration is shown in a plot ($n = 3$ biological replicates) as an internal control of a virus dilution (20, 10 and 5 pfu/well) used if the assay. (**c**) The plot shows TBEV replication dynamic in hBMEC. The dots in the replication curve indicate mean TBEV titer (technical duplicates in two independent biological replications) in medium supernatants collected daily during 10 day-incubation period and tested in viral plaque assay using BHK21 cells. Error bars in the figure denote standard error of mean (SEM).

Isolation of hBMECs proteins

The hBMECs and BT monolayer were washed twice with phosphate buffer saline (PBS, pH 7.4) and scraped. Proteins were isolated under the native conditions and stored at -80 °C until use. Detailed procedure is presented in Supplementary Method S2.

Production of Recombinant domain III TBEV

Gene fragment encoding DIII of the E protein of TBEV (strain Hypr, Slovakia) was PCR amplified (primers and PCR conditions presented in Supplementary Table S2). The nucleotide sequence of the PCR fragment is presented in Supplementary Table S3. The PCR product was cloned into a pQE-30-mCherry-STOP expression vector. Details of vector, digestion, ligation, transformation of *E. coli* M15, protein overexpression, and purification are presented in Supplementary Methods S3 and S4. Methods used to check the purity of rDIII (LDS-PAGE and MALDI-TOF-MS) are described in Supplementary Methods S5 and S6. The concentration of rDIII was measured by the Bradford method. Purified rDIII was stored at − 20 °C in 35% glycerol until use.

Interaction of rDIII and hBMECs

The binding activity of rDIII to hBMECs was evaluated by ELISA and immunocytochemistry. Details of both methods are described in Supplementary Method S7 and S8, respectively.

Mapping of the binding sites on DIII of TBEV interacting with hBMECs

Binding sites on rDIII of TBEV involved in the interactions with hBMECs were identified using the limited tryptic digestion procedure standardized in our previous publication[27]. First, to obtain the tryptic cleavage profile of rDIII, in silico and in solution tryptic digestions were performed as described in Supplementary Method S9 and S10. Putative RBSs on DIII were mapped using on-PVDF membrane limited tryptic digestion approach. Details are presented in Supplementary Method S11.

Production of Recombinant RBSs

Detailed steps of cloning, transformation of *E. coli*, selection of clones, protein overexpression, purification, and quality control are presented in Supplementary Method S12. The concentration of recombinant constructs was measured with NanoDrop One (Thermo Fisher Scientific, Slovakia). Aliquots of purified constructs were vacuum-dried and stored at room temperature until further use.

The N-terminal tag (containing 6xHis-28aa-GGGGS) from RBSs was cleaved with His tagged enterokinase (GenScript Biotech, USA). The purity of the RBSs was checked by MALDI-TOF-MS. Details are presented in Supplementary Method S13.

Confirmation of interaction between RBS and hBMECs

The confirmation of the interaction was necessary to show that: (1) identified peptides are true receptor-binders and are not from any non-specific origin, and (2) the peptides could take part in the formation of the ligand-receptor interface. The interaction between RBSs of rDIII and hBMECs was confirmed by ELISA and immunocytochemistry. Details are presented in Supplementary Method S14.

Localization of the RBS on the crystal structure of DIII of TBEV

To localize the RBSs identified in this study within the DIII sequence, the sequence of rDIII produced in this study was aligned with the amino acid sequence of the E protein of TBEV retrieved from GenBank (U39292.1) using ClustalW (Geneious Pro v 9.1.8; Biomatters, https://www.geneious.com/about). RBSs positions on the E protein were searched in the crystal structure (1SVB) retrieved from the Protein Data Bank in Geneious Pro.

Isolation of peptides displayed on phages possessing binding affinity to RBS

The phage display was employed to isolate peptides from phage libraries interacting with RBSs of rDIII. Two combinatorial phage display peptide libraries (Ph.D.-C7C and Ph.D.-12 Phage Display, New England Biolabs, USA) were panned against rDIII. Several rounds of surface panning were performed using different types of plates and various strategies of phage elution. Please note that in the last round of panning, recombinant RBSs produced above were used for competitive elution of RBS-specific phages. A detailed procedure is described in Supplementary Method S15. Details of each panning are described in Table 1. After the final round of panning, eluted phages were amplified and precipitated. Their binding ability to rDIII was assessed by phage ELISA (details are described in Supplementary Method S16). Phages were then plated on LB agar plates containing 1 mM IPTG (Fermentas, Slovakia) and 1 mM X-gal (Sigma, USA). Thirty well-separated phage plaques were randomly picked and propagated according to the manufacturer's instructions (New England Biolabs, USA) and subjected to sequencing.

Isolation of phage SsDNA, sequencing, and in silico peptide sequence analysis

Genomic ssDNA was isolated by denaturation of each phage clone at 98 °C for 10 min. Sequences encoding phage-displayed 7-mer cyclic and 12-mer linear peptides were amplified with PCR using vector-specific primers (Supplementary Table S2) and sequenced (3100-Advanced Genetic Analyzer). The amino acid sequences were deduced from DNA sequences using Geneious Pro.

The bioinformatics analysis of identified peptide sequences was performed to exclude target-unrelated peptides with the help of the SAROTUP server (http://i.uestc.edu.cn/sarotup3). The Peptide search tool (UniProtKB database, https://www.uniprot.org/peptidesearch) was used to search for possible sequence matches in the public repository.

Round	Solid surface for immobilization of target	Target	Blocking buffer	Amount of phages used to pan (in 100 µL)	Washing buffer	Phage elution
Ph.D.-C7C phage display peptide library						
1st	Pierce™ Nickel Coated Plates	rDIII (0.3 µg/well)	0.1% TBST (pH 7.2) + 1% BSA	2×10^{11} PFU in 0.1% TBST (pH 7.2) + 1% BSA	0.1% TBST (pH 7.2) + 20 mM imidazole	0.1% TBST (pH 7.2) + 250 mM imidazole
2nd	Pierce™ Nickel Coated Plates	rDIII (0.15 µg/well)	0.1% TBST (pH 7.2) + 1% BSA	2×10^{11} PFU in 0.1% TBST (pH 7.2) + 1% BSA	0.1% TBST (pH 7.2) + 20 mM imidazole	0.1% TBST (pH 7.2) + 250 mM imidazole
3rd	Pierce™ Nickel Coated Plates	rDIII (0.3 µg/well)	0.1% TBST (pH 7.2) + 1% BSA	2×10^{9} PFU in 0.1% TBST (pH 7.2) + 1% BSA	0.1% TBST (pH 7.2) + 20 mM imidazole	Competitive elution with RBSs—SGLTYTMCDK and APTDSGHDTVVMEVTFSGTKPCR (1.5 µg) in TBS (pH 7.2)
Ph.D.-12 Phage Display Peptide Library						
1st	Pierce™ Nickel Coated Plates	rDIII (0.3 µg/well)	0.1% TBST (pH 7.2) + 1% BSA	2×10^{11} PFU in 0.1% TBST (pH 7.2) + 1% BSA	0.1% TBST (pH 7.2) + 20 mM imidazole	0.1% TBST (pH 7.2) + 250 mM imidazole
2nd	Pierce™ Nickel Coated Plates	rDIII (0.15 µg/well)	0.1% TBST (pH 7.2) + 1% BSA	2×10^{11} PFU in 0.1% TBST (pH 7.2) + 1% BSA	0.1% TBST (pH 7.2) + 20 mM imidazole	0.1% TBST (pH 7.2) + 250 mM imidazole
3rd	Pierce™ Nickel Coated Plates	rDIII (0.3 µg/well)	0.1% TBST (pH 7.2) + 1% BSA	2×10^{9} PFU in 0.1% TBST (pH 7.2) + 1% BSA	0.1% TBST (pH 7.2) + 20 mM imidazole	Competitive elution with RBSs—SGLTYTMCDK and APTDSGHDTVVMEVTFSGTKPCR (1.5 µg) in TBS (pH 7.2)

Table 1. Description of each round of panning performed to isolate peptides interacting with receptor binding sites on DIII.

Evaluation of the binding ability of individual phage clones to rDIII

Amino acid sequences of the phage-displayed peptides were aligned and grouped based on the sequence homology. Representative phage clones bearing 7-mer cyclic and 12-mer linear peptides were amplified in *E. coli* ER2738 and purified (New England Biolabs). Each phage clone was then evaluated for its ability to bind to rDIII using phage ELISA (Supplementary Method S17). The absorbance > 1.5 was used as a threshold for the selection of peptides for further assessments.

Production of 7-mer Cyclic (CP) and 12-mer linear peptides (LP)

The 7-mer cyclic and 12-mer linear peptides from selected phage clones were produced in the *E. coli* Shuffle express (New England Biolabs) expression system. All peptides were flanked with GGGS sequence at the C-terminus and 7-mer cyclic peptides also with alanine at the N-terminus (ACX_7CGGGS and $X_{12}GGGS$) as suggested by the manufacturer of Ph.D. libraries (New England Biolabs). PCR conditions, digestion, and ligation into the pQE-30-UA-mCherry-STOP expression vector, *E. coli* transformation, clonal selection, protein overexpression, purification, and quality control are presented in Supplementary Method S18. The N-terminal tag (6xHis-28aa-GGGGS tag) was cleaved with bovine Enterokinase (GenScript Biotech) as described in Supplementary Method S13. The purity of the peptides was checked by MALDI-TOF-MS (Supplementary Method S6).

The presence of disulfide bonds in 7-mer cyclic peptides were assessed with thiol-reactive IRDye 800CW Maleimide (LI-COR Biosciences, USA). The disulfide bond ensures a cyclic form of C7C peptides. Details are presented in Supplementary Methods S19 and S20.

Binding of peptides to rDIII

The binding of CPs and LPs to rDIII was evaluated by ELISA. Details are presented in Supplementary Method S21.

Blocking of the interaction between rDIII and proteins of hBMECs with CPs and LPs

First, concentration-dependent ELISA was performed to determine the minimum concentration of rDIII required to show its interaction with hBMECs proteins (Supplementary Method S22). Subsequently, the ability of CPs and LPs to block the interaction between rDIII and proteins of hBMECs was tested. A 10-fold molar excess of peptides was incubated with rDIII for 1 h at room temperature. Pre-incubated rDIII was subsequently added to hBMECs proteins coated in a microtiter well. ELISA was performed to detect a reduction in the binding of rDIII on hBMECs proteins as described in Supplementary Method S22.

Blocking of the adhesion of rDIII on cultured hBMECs

First, concentration-dependent immunocytochemistry was performed to determine the minimum concentration of rDIII required to detect its adhesion to hBMECs. Details are presented in Supplementary Method S23. After that, the ability of peptides to block the adhesion of rDIII to the hBMECs culture was assessed by pre-incubating rDIII with peptides. Details are described in the Supplementary Method S23.

Assessment of peptide cytotoxicity and hemolytic activity

The toxicity of peptides was determined by the XTT (Supplementary Method S24) and a hemolysis assay was performed on sheep red blood cells (Supplementary Method S25).

Neutralization of TBEV by peptides (CP2 and CP20) and blocking of TBEV infection in hBMECs

The primary assessment of CP2 and CP20's ability to neutralize the virus was performed using the virus neutralization test (VNT), in which TBEV (strain Hypr, Slovakia) was preincubated with peptide for 60 min before infecting BHK21 cells. The number of plaques was counted 3 days post-infection (dpi) and compared to the control well that received the virus without pre-incubation. Details are provided in Supplementary Method S26.

Finally, the ability of CP2 and CP20 to inhibit infection in brain microvascular endothelial cells was evaluated by viral plaque reduction assay using the hBMECs and BHK21 cell lines. The assay details are in Supplementary Method S27.

Conclusion

Blocking virus-receptor interactions is a promising concept for restricting cell-entry. The most appropriate approach for drug development aims to target the specific RBSs on viral proteins by mid-sized biomolecules. To our knowledge, this is the first systematic study that focuses on identifying RBSs, synthesizing RBSs, and using them in phage display to generate peptides against RBSs that block viral cell-entry. With limited proteolysis of the rDIII-hBMECs complex, we successfully revealed amino acids stretches $_{300}$SGLTYTMCDK$_{309}$ and $_{317}$APTDSGHDTVVMEVTFSGTKPCR$_{339}$ that are involved in the interface. The involvement of both amino acid stretches in the rDIII-hBMECs interaction was validated, and thus were used for the elution of RBS-specific peptides from phage libraries panned during rounds of selection (biopanning). Among the anti-RBS peptides isolated in this study, cyclic peptides had a higher affinity for rDIII and were more effective at neutralizing the virus. The final shortlisted candidates, CP2 (CNSSKLHMC) and CP20 (CDGRPDRAC) demonstrated no cell toxicity or hemolysis, completely neutralized the virus (1.32 μM), and completely inhibited viral infection in hBMECs at 0.8 nM and 1.7 μM concentration, respectively. We believe that CP2 has the potential to be translated into a peptide-based antiviral agent against TBEV, although further research in this direction is warranted.

Data availability

Data generated in this study are available from the corresponding author upon reasonable request.

Received: 19 November 2024; Accepted: 20 March 2025
Published online: 03 April 2025

References

1. Gritsun, T. S., Lashkevich, V. A. & Gould, E. A. Tick-borne encephalitis. *Antiviral Res.* **57**, 129–146 (2003).
2. Beaute, J., Spiteri, G., Warns-Petit, E. & Zeller, H. Tick-borne encephalitis in Europe, 2012 to 2016. *Euro Surveillance* **23** (2018).
3. Dobler, G. Zoonotic tick-borne flaviviruses. *Vet. Microbiol.* **140**, 221–228 (2010).
4. Wang, L. et al. Therapeutic peptides: Current applications and future directions. *Signal. Transduct. Target. Ther.* **7**, 48 (2022).
5. Al-Azzam, S. et al. Peptides to combat viral infectious diseases. *Peptides* **134**, 170402 (2020).
6. Lee, Y. J., Shirkey, J. D., Park, J., Bisht, K. & Cowan, A. J. An overview of antiviral peptides and rational biodesign considerations. *Biodes. Res.* **2022**, 9898241 (2022).
7. Mazzon, M. & Marsh, M. Targeting viral entry as a strategy for broad-spectrum antivirals. *F1000Res* **8** (2019).
8. Zakaria, M. K., Carletti, T. & Marcello, A. Cellular targets for the treatment of flavivirus infections. *Front. Cell. Infect. Microbiol.* **8**, 398 (2018).
9. Wu, C. H., Liu, I. J., Lu, R. M. & Wu, H. C. Advancement and applications of peptide phage display technology in biomedical science. *J. Biomed. Sci.* **23**, 8 (2016).
10. Castel, G., Chteoui, M., Heyd, B. & Tordo, N. Phage display of combinatorial peptide libraries: Application to antiviral research. *Molecules* **16**, 3499–3518 (2011).
11. Bai, F. et al. Antiviral peptides targeting the West nile virus envelope protein. *J. Virol.* **81**, 2047–2055 (2007).
12. Ozawa, M., Ohashi, K. & Onuma, M. Identification and characterization of peptides binding to Newcastle disease virus by phage display. *J. Vet. Med. Sci.* **67**, 1237–1241 (2005).
13. Ramanujam, P., Tan, W. S., Nathan, S. & Yusoff, K. Novel peptides that inhibit the propagation of Newcastle disease virus. *Arch. Virol.* **147**, 981–993 (2002).
14. Deng, Q. et al. Identification and characterization of peptides that interact with hepatitis B virus via the putative receptor binding site. *J. Virol.* **81**, 4244–4254 (2007).
15. de la Guardia, C., Quijada, M. & Lleonart, R. Phage-displayed peptides selected to bind envelope glycoprotein show antiviral activity against dengue virus serotype 2. *Adv. Virol.* **2017**, 1827341 (2017).
16. Palus, M. et al. Tick-borne encephalitis virus infects human brain microvascular endothelial cells without compromising blood-brain barrier integrity. *Virology* **507**, 110–122 (2017).
17. Ruzek, D., Salat, J., Singh, S. K. & Kopecky, J. Breakdown of the blood-brain barrier during tick-borne encephalitis in mice is not dependent on CD8+ T-cells. *PLoS One* **6**, e20472 (2011).
18. Chen, Y., Maguire, T. & Marks, R. M. Demonstration of binding of dengue virus envelope protein to target cells. *J. Virol.* **70**, 8765–8772 (1996).
19. Lindqvist, R. et al. The envelope protein of tick-borne encephalitis virus influences neuron entry, pathogenicity, and vaccine protection. *J. Neuroinflamm.* **17**, 284 (2020).
20. Rey, F. A., Heinz, F. X., Mandl, C., Kunz, C. & Harrison, S. C. The envelope glycoprotein from tick-borne encephalitis virus at 2 A resolution. *Nature* **375**, 291–298 (1995).
21. Mandl, C. W., Guirakhoo, F., Holzmann, H., Heinz, F. X. & Kunz, C. Antigenic structure of the flavivirus envelope protein E at the molecular level, using tick-borne encephalitis virus as a model. *J. Virol.* **63**, 564–571 (1989).
22. Hung, J. J. et al. An external loop region of domain III of dengue virus type 2 envelope protein is involved in serotype-specific binding to mosquito but not mammalian cells. *J. Virol.* **78**, 378–388 (2004).
23. Li, C. et al. Inhibition of Japanese encephalitis virus entry into the cells by the envelope glycoprotein domain III (EDIII) and the loop3 peptide derived from EDIII. *Antiviral Res.* **94**, 179–183 (2012).

24. Chu, J. J. H. et al. Inhibition of West nile virus entry by using a recombinant domain III from the envelope glycoprotein. *J. Gen. Virol.* **86**, 405–412 (2005).
25. Roehrig, J. T. et al. Mutation of the dengue virus type 2 envelope protein heparan sulfate binding sites or the domain III lateral ridge blocks replication in vero cells prior to membrane fusion. *Virology* **441**, 114–125 (2013).
26. Crill, W. D. & Roehrig, J. T. Monoclonal antibodies that bind to domain III of dengue virus E glycoprotein are the most efficient blockers of virus adsorption to vero cells. *J. Virol.* **75**, 7769–7773 (2001).
27. Mertinkova, P. et al. A simple and rapid pipeline for identification of receptor-binding sites on the surface proteins of pathogens. *Sci. Rep.* **10**, 1163 (2020).
28. Bhide, K. et al. Signaling events evoked by domain III of envelop glycoprotein of tick-borne encephalitis virus and West nile virus in human brain microvascular endothelial cells. *Sci. Rep.* **12**, 8863 (2022).
29. Mandl, C. W., Allison, S. L., Holzmann, H., Meixner, T. & Heinz, F. X. Attenuation of tick-borne encephalitis virus by structure-based site-specific mutagenesis of a putative flavivirus receptor binding site. *J. Virol.* **74**, 9601–9609 (2000).
30. Liu, H. et al. Structure-based mutational analysis of several sites in the E protein: Implications for understanding the entry mechanism of Japanese encephalitis virus. *J. Virol.* **89**, 5668–5686 (2015).
31. Holzmann, H., Stiasny, K., Ecker, M., Kunz, C. & Heinz, F. X. Characterization of monoclonal antibody-escape mutants of tick-borne encephalitis virus with reduced neuroinvasiveness in mice. *J. Gen. Virol.* **78** (Pt 1), 31–37 (1997).
32. Holzmann, H., Heinz, F. X., Mandl, C. W., Guirakhoo, F. & Kunz, C. A single amino acid substitution in envelope protein E of tick-borne encephalitis virus leads to attenuation in the mouse model. *J. Virol.* **64**, 5156–5159 (1990).
33. Lee, E. & Lobigs, M. Substitutions at the putative receptor-binding site of an encephalitic flavivirus alter virulence and host cell tropism and reveal a role for glycosaminoglycans in entry. *J. Virol.* **74**, 8867–8875 (2000).
34. Mandl, C. W. et al. Adaptation of tick-borne encephalitis virus to BHK-21 cells results in the formation of multiple Heparan sulfate binding sites in the envelope protein and attenuation in vivo. *J. Virol.* **75**, 5627–5637 (2001).
35. Wei, J. et al. Antiviral activity of phage display-selected peptides against Japanese encephalitis virus infection in vitro and in vivo. *Antiviral Res.* **174**, 104673 (2020).
36. Zu, X. et al. Peptide inhibitor of Japanese encephalitis virus infection targeting envelope protein domain III. *Antiviral Res.* **104**, 7–14 (2014).
37. Mertinkova, P. et al. Development of peptides targeting receptor binding site of the envelope glycoprotein to contain the West nile virus infection. *Sci. Rep.* **11**, 20131 (2021).
38. Gho, Y. S., Lee, J. E., Oh, K. S., Bae, D. G. & Chae, C. B. Development of antiangiogenin peptide using a phage-displayed peptide library. *Cancer Res.* **57**, 3733–3740 (1997).
39. O'Neil, K. T. et al. Identification of novel peptide antagonists for GPIIb/IIIa from a conformationally constrained phage peptide library. *Proteins* **14**, 509–515 (1992).
40. Ho, K. L., Yusoff, K., Seow, H. F. & Tan, W. S. Selection of high affinity ligands to hepatitis B core antigen from a phage-displayed cyclic peptide library. *J. Med. Virol.* **69**, 27–32 (2003).
41. Tan, W. S., Tan, G. H., Yusoff, K. & Seow, H. F. A phage-displayed cyclic peptide that interacts tightly with the immunodominant region of hepatitis B surface antigen. *J. Clin. Virol.* **34**, 35–41 (2005).
42. Luo, H. B., Zheng, S. G., Zhu, P. & Fu, N. Study on mimotopes of *E. coli* lipopolysaccharide 2630. *J. Cell. Mol. Immunol.* **20**, 682–685 (2004).
43. Lowman, H. B. Bacteriophage display and discovery of peptide leads for drug development. *Annu. Rev. Biophys. Biomol. Struct.* **26**, 401–424 (1997).
44. Haug, B. E., Stensen, W., Kalaaji, M., Rekdal, O. & Svendsen, J. S. Synthetic antimicrobial peptidomimetics with therapeutic potential. *J. Med. Chem.* **51**, 4306–4314 (2008).
45. Matsuzaki, K. Control of cell selectivity of antimicrobial peptides. *Biochim. Biophys. Acta* **1788**, 1687–1692 (2009).
46. Amin, K. & Dannenfelser, R. M. In vitro hemolysis: Guidance for the pharmaceutical scientist. *J. Pharm. Sci.* **95**, 1173–1176 (2006).
47. Mladinich, M. C., Schwedes, J. & Mackow, E. R. Zika virus persistently infects and is basolaterally released from primary human brain microvascular endothelial cells. *mBio* **8** (2017).
48. Friedman, M. G., Phillip, M. & Dagan, R. Virus-specific IgA in serum, saliva, and tears of children with measles. *Clin. Exp. Immunol.* **75**, 58–63 (1989).
49. Papa, M. P. et al. Zika virus infects, activates, and crosses brain microvascular endothelial cells, without barrier disruption. *Front. Microbiol.* **8**, 2557 (2017).
50. Chen, L. et al. Antiviral activity of peptide inhibitors derived from the protein E stem against Japanese encephalitis and Zika viruses. *Antiviral Res.* **141**, 140–149 (2017).
51. Galdiero, S. et al. Peptide inhibitors against herpes simplex virus infections. *J. Pept. Sci.* **19**, 148–158 (2013).
52. Mears, M. C. et al. Design and evaluation of neutralizing and fusion inhibitory peptides to Crimean-Congo hemorrhagic fever virus. *Antiviral Res.* **207**, 105401 (2022).
53. Beckham, J. D., Goody, R. J., Clarke, P., Bonny, C. & Tyler, K. L. Novel strategy for treatment of viral central nervous system infection by using a cell-permeating inhibitor of c-Jun N-terminal kinase. *J. Virol.* **81**, 6984–6992 (2007).
54. Yu, L. et al. Delineating antibody recognition against Zika virus during natural infection. *JCI Insight* **2** (2017).
55. Austin, S. K. et al. Structural basis of differential neutralization of DENV-1 genotypes by an antibody that recognizes a cryptic epitope. *PLoS Pathog.* **8**, e1002930 (2012).
56. Li, C. et al. A single injection of human neutralizing antibody protects against Zika virus infection and microcephaly in developing mouse embryos. *Cell. Rep.* **23**, 1424–1434 (2018).
57. Niu, X. et al. Convalescent patient-derived monoclonal antibodies targeting different epitopes of E protein confer protection against Zika virus in a neonatal mouse model. *Emerg. Microbes Infect.* **8**, 749–759 (2019).
58. Shrestha, B. et al. The development of therapeutic antibodies that neutralize homologous and heterologous genotypes of dengue virus type 1. *PLoS Pathog.* **6**, e1000823 (2010).
59. Wang, J. et al. A human bi-specific antibody against Zika virus with high therapeutic potential. *Cell* **171**, 229–241 e215 (2017).
60. Wang, L. et al. Structural basis for neutralization and protection by a Zika virus-specific human antibody. *Cell. Rep.* **26**, 3360–3368e3365 (2019).
61. Lin, Y. et al. Mapping of the B cell neutralizing epitopes on ED III of envelope protein from dengue virus. *Bing Du Xue Bao.* **31**, 665–673 (2015).
62. Tabata, T. et al. Zika virus targets different primary human placental cells, suggesting two routes for vertical transmission. *Cell. Host Microbe.* **20**, 155–166 (2016).
63. Alagarasu, K. et al. In-vitro effect of human cathelicidin antimicrobial peptide LL-37 on dengue virus type 2. *Peptides* **92**, 23–30 (2017).
64. Li, F. et al. A scorpion venom peptide Ev37 restricts viral late entry by alkalizing acidic organelles. *J. Biol. Chem.* **294**, 182–194 (2019).
65. Monteiro, J. M. C. et al. The antimicrobial peptide HS-1 inhibits dengue virus infection. *Virology* **514**, 79–87 (2018).
66. Panya, A. et al. A synthetic bioactive peptide derived from the Asian medicinal plant acacia Catechu binds to dengue virus and inhibits cell entry. *Viruses* **12** (2020).

Acknowledgements
The authors thank Ing. Martina Cepkova and Ing. Viera Rusnakova for their technical assistance. Research was funded by grants APVV-22-0084, APVV-18-0259, APVV-23-0348, VEGA1/0381/23, VEGA1/0348/22 and EURONANOMED2021-105.

Author contributions
MB and JK designed experiments. PP, EM and ZT performed phage display, panning, overexpression of proteins and peptide purification, ELISA, XTT and hemolysis assays. PP performed blocking ELISA and cytochemistry. PP and A. Kulkarni performed RBS mapping experiments. KB and MB performed steps in RNA isolation from the strain Hypr, cDNA synthesis, and primer design for amplification of DIII. A cell culture studies were performed by KB and ÁK. JJ, TM, KB, K. Kucková, LT and JV performed VNT experiments in BSL-3 facility. ÁK, K. Koči, EN and JK performed a virus infection dynamics study and blocking of hBMEC infection by peptides. Statistical and bioinformatic analyses were performed by PP, EM and MB. PP, JK, and MB prepared the manuscript. All authors approved the final version of the manuscript.

Declarations

Competing interests
The authors declare no competing interests.

Additional information
Supplementary Information The online version contains supplementary material available at https://doi.org/10.1038/s41598-025-95449-1.

Correspondence and requests for materials should be addressed to J.K. or M.B.